

Comparison of fractional anisotropy and apparent diffusion coefficient among hypoxic ischemic encephalopathy stages 1, 2, and 3 and with nonasphyxiated newborns in 18 areas of brain

Supriya Kushwah, Ashok Kumar¹, Ashish Verma¹, Sriparna Basu¹, Ashutosh Kumar²

Department of Paediatrics, Yenepoya Medical College, ²Department of Anaesthesia, KMC, Mangalore, Karnataka, ¹Department of Paediatrics, Institute of Medical Sciences, Varanasi, Uttar Pradesh, India

Correspondence: Dr. Supriya Kushwah, Department of Paediatrics, Yenepoya Medical College, Mangalore, Karnataka, India.
E-mail: drsupriyabhu@gmail.com

Abstract

Purpose: To determine the area and extent of injury in hypoxic encephalopathy stages by diffusion tensor imaging (DTI) using parameters apparent diffusion coefficient (ADC) and fractional anisotropy (FA) values and their comparison with controls without any evidence of asphyxia. To correlate the outcome of hypoxia severity clinically and significant changes on DTI parameter. **Materials and Methods:** DTI was done in 50 cases at median age of 12 and 20 controls at median age of 7 days. FA and apparent diffusion coefficient (ADC) were measured in several regions of interest (ROI). Continuous variables were analyzed using Student's *t*-test. Categorical variables were compared by Fisher's exact test. Comparison among multiple groups was done using analysis of variance (ANOVA) and *post hoc* Bonferroni test. **Results:** Abnormalities were more easily and accurately determined in ROI with the help of FA and ADC values. When compared with controls FA values were significantly decreased and ADC values were significantly increased in cases, in ROI including both right and left side of thalamus, basal ganglia, posterior limb of internal capsule, cerebral peduncle, corticospinal tracts, frontal, parietal, temporal, occipital with *P* value < 0.05. The extent of injury was maximum in stage-III. There was no significant difference among males and females. **Conclusion:** Compared to conventional magnetic resonance imaging (MRI), the evaluation of FA and ADC values using DTI can determine the extent and severity of injury in hypoxic encephalopathy. It can be used for early determination of brain injury in these patients.

Key words: Apparent diffusion coefficient; diffusion tensor imaging; fractional anisotropy; hypoxic ischemic encephalopathy

Introduction

Neonatal encephalopathy associated with perinatal hypoxia-ischemia has been one of the leading causes

of neonatal mortality and permanent neurological disability worldwide. Moderate to severe hypoxic ischemic encephalopathy (HIE) occurs at a rate of approximately

This is an open access article distributed under the terms of the Creative Commons Attribution-NonCommercial-ShareAlike 3.0 License, which allows others to remix, tweak, and build upon the work non-commercially, as long as the author is credited and the new creations are licensed under the identical terms.

For reprints contact: reprints@medknow.com

Cite this article as: Kushwah S, Kumar A, Verma A, Basu S, Kumar A. Comparison of fractional anisotropy and apparent diffusion coefficient among hypoxic ischemic encephalopathy stages 1, 2, and 3 and with nonasphyxiated newborns in 18 areas of brain. Indian J Radiol Imaging 2017;27:447-56.

Access this article online

Quick Response Code:



Website:
www.ijri.org

DOI:
10.4103/ijri.IJRI_384_16

1–2 per 1,000 term live births^[1,2] with a total HIE incidence of 3–5 cases per 1,000 term live births.^[3] Lawn *J et al.*, 2005 found the incidence is up to 10-fold higher in developing countries and globally, 23% of the 4 million annual neonatal deaths are attributed to birth asphyxia. Perinatal asphyxia is believed to account for 10–20% of cases of cerebral palsy^[4] and 30% risk of disabilities including blindness, deafness, autism, epilepsy, global developmental delay, and problems with cognition, memory, fine motor skills, and behavior.^[5]

Various neuroimaging studies, i.e., magnetic resonance imaging (MRIs) are well-known to know the extent of injury in HIE. Recently, newer techniques such as diffusion-weighted imaging (DWI) and diffusion tensor MRI (DTMRI) have been proved to be more sensitive than conventional MRI to explore brain development and white matter (WM) fibers density and maturation.^[6–8] Tractography is performed in DTMRI and the findings are expressed in colored 3D shape. In normal brain, free diffusion of water occurs equally in all directions, termed as “isotropic” diffusion. If the water diffuses in a medium with barriers, the diffusion becomes uneven, which is termed “anisotropic” diffusion. Anisotropy is measured in several ways. One way is by a ratio called fractional anisotropy (FA).

Dynamic changes of FA and trace may be explained by concomitant maturation-induced changes in tissue microstructure, such as reduction in water content, greater cohesiveness of fiber tracts or fiber organization, maturation of axons, and myelination. Conditions where the myelin or the structure of the axon are disrupted, such as trauma, tumors, and inflammation are known to reduce anisotropy, as the barriers are affected by destruction or disorganization. Apparent diffusion coefficient (ADC) is defined as the ratio of mean-squared displacement and the diffusion time. Both of these values are important to assess brain damage.^[9] Therefore, it is also useful to identify a noninvasive method to detect and monitor the evolution of HI-induced damage for treatment selection and to determine the effectiveness of treatment.

There is limited experience of using DTMRI in different areas of brain in perinatal asphyxia, though several studies have shown changes in HIE. DWI is a better modality to correlate the outcome of asphyxiated babies. This study was conducted to determine the area and extent of injury in hypoxic encephalopathy stages by diffusion tensor imaging (DTI) using parameters apparent diffusion coefficient (ADC) and FA values and their comparison with controls without any evidence of asphyxia. Outcome of hypoxia severity clinically and significant changes on DTI parameter was also determined.

Materials and Methods

This prospective observational study was conducted in the Department of Pediatrics and the Department of Radiology,

Institute of Medical Sciences, Banaras Hindu University. The period of study extended from December 2011 to July 2013. Informed consent was taken from all parents before inclusion in the study. The study was approved by the Institute Ethics Committee.

Inclusion criteria

The study population comprised of term newborns (37–41 weeks) who suffered perinatal asphyxia. Perinatal asphyxia was defined as the need for delivery room resuscitation and development of clinical manifestations suggestive of HIE. Both inborn and outborn babies were included. Control group comprised of newborns were evaluated for possible sepsis, but had negative laboratory work up including blood culture.

Exclusion criteria

Newborns with sepsis, respiratory distress, metabolic disorders, and major congenital malformations were excluded from the study.

Newborns were managed as per unit protocol. Progression of HIE into different stages was categorized according to the classification of Fenichel.^[10] DTMRI was done using 1.5 Tesla MRI Magnetom Avanto (Version; BV-I7A) Siemens medical system, Erlangen, Germany, between D5 and D20 of life in those who survived. Straps and bolsters were used to help the infants stay still and maintain the correct position during imaging. Lorazepam at 0.05 mg/kg/dose was used to sedate the infants. The protocol consisted of high resolution anatomical images acquired with a T1-weighted sagittal three-dimension (3D) magnetization-prepared rapid gradient-echo (MPRAGE) sequence [TR 7.1, TE 3.45ms, TI 1000ms, and flip angle 7 degrees, field of view (FOV) 256 mm × 256 mm, and slab thickness 150 mm]. The acquisition matrix was 256 × 192 × 128, reconstructed voxel resolution of 1.0 mm × 1.0 mm × 1.33 mm. The DTI sequence was a single shot balanced echo planar imaging (EPI) sequence with timing parameters of TR 6000 ms and TE 97 ms. The 20 contiguous transverse slices with a slice thickness of 5 mm were aligned parallel to the anterior commissure and posterior commissure plane and covered all, but the topmost part of the brain. The FOV was 128 mm × 128 mm, acquisition matrix 96 × 128, reconstructed to 128 × 128, giving a reconstructed in-plane resolution of 1.78 mm × 1.78 mm. For each slice, one image without diffusion weighting ($b = 0$ s/mm square) and six images with diffusion weighting ($b_0 = 1000$ s/mm square) applied along six non-collinear directions were acquired. The six DTI acquisitions for each subject were registered using a mutual information cost function and a 12 parameter affine transformation with the first $b = 0$ s/mm square volume reference.

Data post-processing was done using the automated Neuro-3D software (Siemens Medical System, Erlangen,

Germany) on the off line workstation. Quantitative analysis was done by drawing region of interest (ROI) following a pre-standardized protocol in the interactive maps generated by the software to include the WM tracts emanating from most functionally active areas in the brain. FA and ADC were measured in several ROI in brain including both right and left side of thalamus, basal ganglia, posterior limb of internal capsule, cerebral peduncle, corticospinal tracts, frontal, parietal, temporal, and occipital.

Results

The study population comprised of 50 term newborns with HIE as cases and 20 term newborns as controls. Among cases, 8 (16%) neonates progressed up to HIE stage I, 6 (12%) up to stage HIE II, and 36 (72%) up to stage HIE III. During hospital stay, 16 (32%) neonates with HIE expired. Among cases, the incidence of HIE stage III was significantly higher in unbooked mothers ($P < 0.01$) and in extramural deliveries ($P < 0.01$). There was no statistical difference in gravidity, parity, gestation, birth weight, sex, mode of delivery, and birth through meconium stained amniotic fluid (MSAF) among three stages of HIE [Table 1]. Neuroimaging findings were suggestive of more damage in higher stages of HIE [Figure 1]. Figure 2 is suggestive of diffuse damage to brain with abnormal diffusion and abnormal myelination. FA was significantly reduced and ADC was significantly increased in HIE in all areas (ROI) compared to controls [Table 2]. In boxplot number 1–18 denotes different areas respectively as follows: 1. Right thalamus 2. Left thalamus 3. Right basal ganglia 4. Left basal ganglia 5. Right posterior limb of internal capsule

6. Left posterior limb of internal capsule 7. Right cerebral peduncle 8. Left cerebral peduncle 9. Right corticospinal tracts 10. Left corticospinal tracts 11. Right frontal 12. Left frontal 13. Right parietal 14. Left parietal 15. Right temporal 16. Left temporal 17. Right occipital 18. Left occipital. Boxplot 1 and 2 is suggestive of that FA was low in cases as compared to controls and there was a variation of FA in cases was due to varying ischemic insult among HIE. Boxplot 3 and 4 suggested that ADC was comparatively higher in cases as compared to controls.

Statistical analysis was done using the SPSS version 16.0 (NY, USA). Data was expressed as mean \pm standard deviation for continuous variables and percentage for categorical variables. Continuous variables were analyzed using Student's *t*-test or Mann-Whitney U-test as applicable. Categorical variables were compared by Fisher's exact

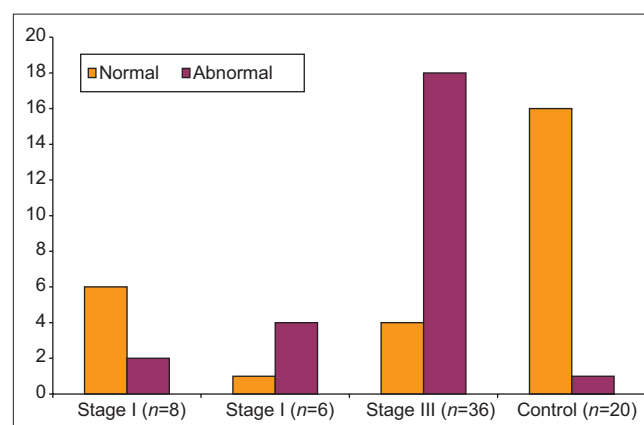


Figure 1: An incidence of abnormal DTMRI in HIE compared to controls

Table 1: Baseline characteristics of the study population

Parameters	Case (n=50)			Control (n=20)	Comparison between cases and controls (P)
	Stage I (n=8)	Stage II (n=6)	Stage III (n=36)		
Maternal					0.012
Booked	3 (37.5%)	6 (100%)	10 (27.77%)	12 (60%)	
Unbooked	5 (62.5%)	0 (0%)	26 (72.22%)	8 (40%)	
Gravida					0.645 (NS)
Median	1	1	1	1	
Parity					0.452 (NS)
Median	1	1	1	1	
Birth weight (g)	2800 \pm 460	2883 \pm 365	2788 \pm 342	2830 \pm 435	0.139 (NS)
GA (wk)	37.5 \pm 1.1	37.8 \pm 1.2	37.8 \pm 1.3	38.2 \pm 1.1	0.514 (NS)
Delivery					0.024
Intramural	4 (50%)	1 (16.67%)	2 (5.56%)	8 (40%)	
Extramural	4 (50%)	5 (83.33%)	34 (94.44%)	12 (60%)	
Mode of delivery					0.042
SVD	6 (75%)	5 (83.33%)	29 (80.56%)	11 (55%)	
Cesarean section	2 (25%)	1 (16.67%)	7 (19.44%)	9 (45%)	
Sex					0.778 (NS)
Male	6 (75%)	5 (83.33%)	24 (66.67%)	13 (65%)	
Female	2 (25%)	1 (16.67%)	12 (33.33%)	7 (35%)	

SVD: Spontaneous vaginal delivery

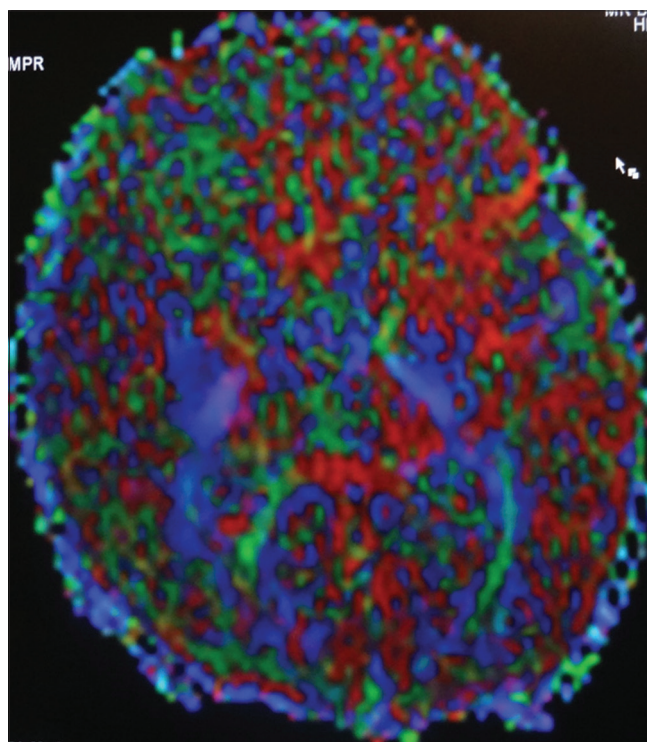
Table 2: Diffusion tensor magnetic resonance imaging in study groups

Parameter	Cases (n=29)	Controls (n=17)	P
Thalamus			
Right			
Fractional anisotropy	201.55±64.39	262.49±51.31	P<0.05
Apparent diffusion coefficient	979.60±206.29	842.81±61.31	P<0.05
Left			
Fractional anisotropy	194.27±56.52	279.89±64.03	P<0.001
Apparent diffusion coefficient	1023.71±121.35	838.81±50.64	P<0.001
Basal ganglia			
Right			
Fractional anisotropy	145.30±48.06	179.96±67.61	P<0.05
Apparent diffusion coefficient	1070.41±140.00	849.18±84.28	P<0.001
Left			
Fractional anisotropy	153.04±47.70	192.46±69.00	P<0.05
Apparent diffusion coefficient	1070.46±149.02	854.42±61.68	P<0.001
Posterior limb of internal capsule			
Right			
Fractional anisotropy	398.28±151.70	590.89±108.42	P<0.001
Apparent diffusion coefficient	972.54±134.25	835.66±62.43	P<0.001
Left			
Fractional anisotropy	433.10±120.69	621.62±115.47	P<0.001
Apparent diffusion coefficient	989.71±129.39	824.69±65.96	P<0.001
Cerebral peduncle			
Right			
Fractional anisotropy	220.29±57.48	363.54±121.78	P<0.001
Apparent diffusion coefficient	986.45±120.45	809.45±175.62	P<0.001
Left			
Fractional anisotropy	234.95±57.86	320.84±113.35	P<0.05
Apparent diffusion coefficient	997.48±99.42	814.56±99.85	P<0.001
Corticospinal tracts			
Right			
Fractional anisotropy	257.61±107.56	381.82±132.92	P<0.05
Apparent diffusion coefficient	1340.50±235.29	920.45±111.97	P<0.001
Left			
Fractional anisotropy	263.18±120.66	400.97±134.47	P<0.05
Apparent diffusion coefficient	1306.26±184.26	906.46±92.99	P<0.001
Frontal			
Right			
Fractional anisotropy	180.27±81.63	335.95±142.75	P<0.001
Apparent diffusion coefficient	1393.17±469.95	877.35±148.80	P<0.001
Left			
Fractional anisotropy	168.28±90.49	314.40±103.59	P<0.001
Apparent diffusion coefficient	1254.21±295.94	825.66±94.18	P<0.001
Parietal			
Right			
Fractional anisotropy	163.50±51.43	232.17±78.06	P<0.05
Apparent diffusion coefficient	1316.00±313.61	881.89±99.15	P<0.001
Left			
Fractional anisotropy	152.44±69.71	249.95±71.12	P<0.001
Apparent diffusion coefficient	1304.19±223.35	875.05±131.47	P<0.001

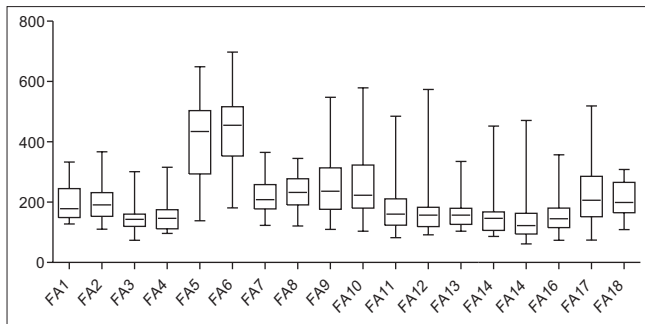
Contd...

Table 2: Contd...

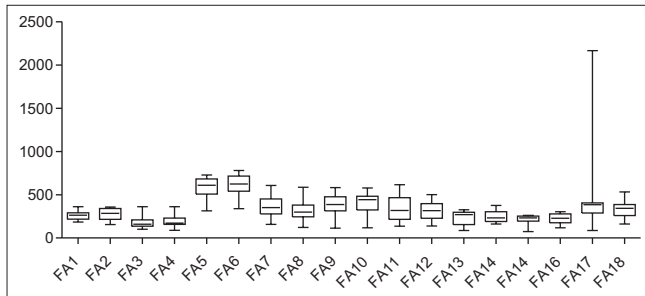
Parameter	Cases (n=29)	Controls (n=17)	P
Temporal			
Right			
Fractional anisotropy	140.07±78.40	214.78±51.52	P<0.05
Apparent diffusion coefficient	1254.61±321.33	892.59±63.16	P<0.001
Left			
Fractional anisotropy	151.89±60.69	220.72±57.99	P<0.001
Apparent diffusion coefficient	1353.31±281.73	889.62±59.95	P<0.001
Occipital			
Right			
Fractional anisotropy	217.31±100.39	449.24±457.12	P<0.05
Apparent diffusion coefficient	1306.91±240.08	848.16±126.46	P<0.001
Left			
Fractional anisotropy	209.37±57.75	329.85±94.07	P<0.001
Apparent diffusion coefficient	1297.22±229.00	913.65±78.52	P<0.001

**Figure 2:** Baseline characteristics of the study population

test. Comparison among multiple groups was done using analysis of variance (ANOVA) and *post hoc* Bonferroni test. Pearson correlation coefficient was calculated for different variables. *P* value of <0.05 was considered statistically significant. There was statistically significant difference in FA between controls and cases, except in left basal ganglia, left cerebral peduncle, left parietal, right occipital and ADC, except in left thalamus and right posterior limb of internal capsule [Table 3]. The extent of neuronal injury was maximum in stage III HIE. When compared with controls significant decrease in FA was observed in right



Boxplot 1: Fractional anisotropy in study group



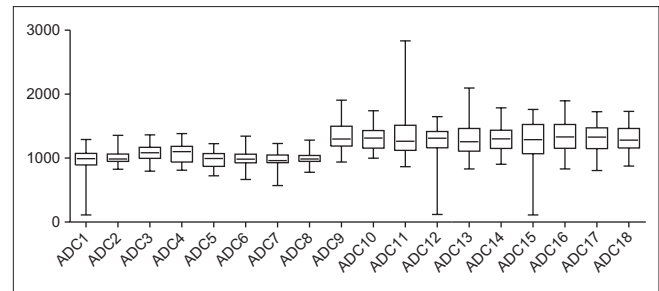
Boxplot 3: Fractional anisotropy in control group

thalamus, right basal ganglia, bilateral posterior limb of internal capsule, cerebral peduncle, corticospinal tracts, frontal, right parietal, and right temporal region. ADC values were significantly higher in left thalamus, bilateral basal ganglia, right corticospinal tracts, bilateral frontal, parietal, temporal, and occipital areas. Between controls and stage I, FA was significantly reduced in right posterior limb of internal capsule and right cerebral peduncle. Between controls and stage II, significant increase in ADC was seen in corticospinal tracts, temporal and occipital of both sides. When compared between stage I and stage III significant difference in FA was seen in left thalamus and bilateral temporal. Significant difference in ADC was seen in right corticospinal tracts, bilateral parietal, temporal, and occipital areas [Table 4]. We did not find any significant difference among males and females in DTI.

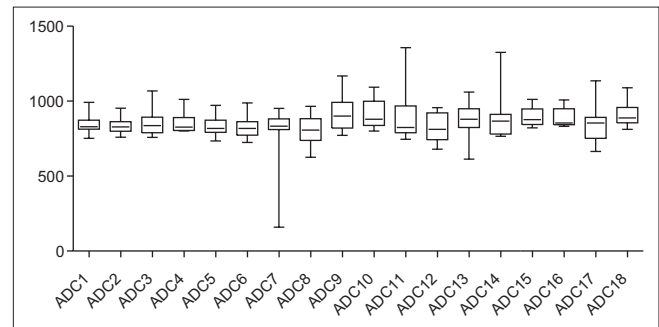
Discussion

Severe brain injury is characterized by tissue loss and necrosis in both WM and gray matter, mild injury leads predominantly to WM damage. Such selective WM damage in mild hypoxia-ischemia may be due to apoptosis of immature oligodendrocyte progenitors and dysfunction of mature oligodendrocytes, which are susceptible to HI injury.^[11-13]

DTMRI was used to delineate the pattern of brain injury in perinatal asphyxia at median age of 7 days in controls and 12 days in cases. A significant decrease in FA and increase in ADC was documented in all ROI studied (both right and left side of thalamus, basal ganglia, posterior limb of



Boxplot 2: Apparent diffusion coefficient in study group



Boxplot 4: Apparent diffusion coefficient in control group

internal capsule, cerebral peduncle, corticospinal tracts, frontal, parietal, temporal, and occipital) in HIE, compared to controls.

We did not find any study in which FA and ADC in different ROI were compared among stages of HIE. Among control and stage I, FA was significantly decreased in right posterior limb of internal capsule and right cerebral peduncle. Among control and stage II, significant increase in ADC was seen in corticospinal tracts, temporal and occipital of both sides. Thus, we also found difference in neuronal injury in left and right side. Stage III showed maximum extent of injury. When compared with controls, significant decrease in FA was observed in right thalamus, right basal ganglia, bilateral posterior limb of internal capsule, cerebral peduncle, corticospinal tracts, frontal, right parietal, and right temporal region, whereas significantly higher ADC values were observed in left thalamus, bilateral basal ganglia, right corticospinal tracts, bilateral frontal, parietal, temporal, and occipital areas.

When compared between stage I and stage III, significant difference was observed in FA in left thalamus, bilateral temporal and ADC in right corticospinal tracts, bilateral parietal, temporal, and occipital areas.

Brain WM myelination is a long process which starts well before birth and continues until adulthood. Postmortem studies have shown that myelination progresses in a caudo-rostral way, at different rates depending on location,^[14-17] with earlier maturation of motor and sensory tracts in comparison with cortico-tracts association fibers.

Table 3: Comparison of fractional anisotropy and apparent diffusion coefficient among controls and study groups

Parameter	Controls (<i>n</i> =17)	HIE Stage I (<i>n</i> =7)	HIE Stage II (<i>n</i> =5)	HIE Stage III (<i>n</i> =17)	ANOVA	
					<i>F</i>	<i>P</i>
Thalamus						
Right						
Fractional anisotropy	262.49±51.31	244.1±70.79	209.78±57.13	186.08±62.19	5.08	<i>P</i> <0.05
Apparent diffusion coefficient	842.81±61.31	814.9±369.55	1064.7±120.9	944.24±236.29	2.10	NS
Left						
Fractional anisotropy	279.89±64.03	339.44±259.28	195.5±21.98	181.06±51.98	4.49	<i>P</i> <0.05
Apparent diffusion coefficient	838.81±50.64	826.89±376.86	1056.54±179.77	1018.85±92.49	5.19	<i>P</i> <0.05
Basal ganglia						
Right						
Fractional anisotropy	179.96±67.61	154.86±19.59	170.34±35.04	121.96±29.39	4.50	<i>P</i> <0.05
Apparent diffusion coefficient	849.18±84.28	891.63±387.32	1074.22±156.82	1081.19±151.48	5.25	<i>P</i> <0.05
Left						
Fractional anisotropy	192.46±69.00	256.23±252.45	145.12±26.4	141.36±39.89	2.15	NS
Apparent diffusion coefficient	854.42±61.68	884.59±421.74	1000.04±143.5	1104.26±131.49	5.54	<i>P</i> <0.05
Posterior limb of internal capsule						
Right						
Fractional anisotropy	590.89±108.42	365.69±143.42	521.76±114.44	371.39±138.09	10.53	<i>P</i> <0.001
Apparent diffusion coefficient	835.66±62.43	845.31±380.03	1000.26±104.67	953.8±138.82	2.08	NS
Left						
Fractional anisotropy	621.62±115.47	501.01±210.22	497.06±125.73	417.86±100.62	7.10	<i>P</i> <0.05
Apparent diffusion coefficient	824.69±65.96	827.51±411.19	995.6±100.48	987.95±85.38	3.49	<i>P</i> <0.05
Cerebral peduncle						
Right						
Fractional anisotropy	363.54±121.78	229.86±50.08	256.3±89.8	203.81±44.18	10.43	<i>P</i> <0.001
Apparent diffusion coefficient	809.45±175.62	838.24±385.86	1035.1±76.55	971.71±130.46	2.87	<i>P</i> <0.05
Left						
Fractional anisotropy	320.84±113.35	316.03±223.79	290.28±67.23	213.52±49.63	2.80	NS
Apparent diffusion coefficient	814.56±99.85	837.87±413.55	1012.16±47.03	977.84±82.42	3.41	<i>P</i> <0.05
Corticospinal tracts						
Right						
Fractional anisotropy	381.82±132.92	306.74±163.61	315.88±135.18	236.74±84.92	3.97	<i>P</i> <0.05
Apparent diffusion coefficient	920.45±111.97	1044.46±483.13	1307.52±160.14	1390.26±238.27	11.14	<i>P</i> <0.001
Left						
Fractional anisotropy	400.97±134.47	332.06±220.88	280.1±121.26	255.01±118.91	3.10	<i>P</i> <0.05
Apparent diffusion coefficient	906.46±92.99	1056.61±534.58	1308.4±173.03	1327.14±152.08	10.20	<i>P</i> <0.001
Frontal						
Right						
Fractional anisotropy	335.95±142.75	248.47±175.22	192.3±103.02	182.33±87.96	4.56	<i>P</i> <0.05
Apparent diffusion coefficient	877.35±148.80	996.99±438.59	1085.72±120.55	1526.56±551.04	8.40	<i>P</i> <0.001
Left						
Fractional anisotropy	314.40±103.59	257.56±241.46	197.88±81.46	168.44±108.67	3.65	<i>P</i> <0.05
Apparent diffusion coefficient	825.66±94.18	1016.64±474.39	984.86±547.78	1318.38±189.82	9.03	<i>P</i> <0.001
Parietal						
Right						
Fractional anisotropy	232.17±78.06	167.9±59.85	179.66±54.72	164.96±57.16	3.41	<i>P</i> <0.05
Apparent diffusion coefficient	881.89±99.15	1000.74±436.14	1216.64±216.91	1386.56±350.22	9.41	<i>P</i> <0.001
Left						
Fractional anisotropy	249.95±71.12	244.19±281.06	153.96±30.5	160.96±85.3	1.89	NS
Apparent diffusion coefficient	875.05±131.47	898.39±400.59	1241.4±272.81	1384.24±195.23	17.06	<i>P</i> <0.001

Contd...

Table 3: Contd...

Parameter	Controls (n=17)	HIE Stage I (n=7)	HIE Stage II (n=5)	HIE Stage III (n=17)	ANOVA	
					F	P
Temporal						
Right						
Fractional anisotropy	214.78±51.52	216±136.73	154.54±54.93	116.17±39.56	7.24	P<0.05
Apparent diffusion coefficient	892.59±63.16	930.06±410.98	1304.04±306.4	1332.79±224.77	12.76	P<0.001
Left						
Fractional anisotropy	220.72±57.99	296.7±279.59	153.4±38.16	135.44±44.86	3.81	P<0.05
Apparent diffusion coefficient	889.62±59.95	998.81±450.83	1311.86±399.03	1416.28±262.53	12.29	P<0.001
Occipital						
Right						
Fractional anisotropy	449.24±457.12	297.97±129.59	280.4±151.83	193.04±93.39	2.16	NS
Apparent diffusion coefficient	848.16±126.46	973.46±461.67	1270.82±306.95	1365.92±213.52	13.45	P<0.001
Left						
Fractional anisotropy	329.85±94.07	328.14±315.42	241.42±50.96	199.31±60.76	3.01	P<0.05
Apparent diffusion coefficient	913.65±78.52	944.14±460.96	1256.62±240.72	1373.14±195.1	13.41	P<0.001

ANOVA: Analysis of variance, HIE: Hypoxic ischemic encephalopathy

Table 4: Comparison between controls and study groups

Parameter	Control vs. Stage I	Control vs. Stage II	Control vs. Stage III	Stage I vs. Stage II	Stage I vs. Stage III	Stage II vs. Stage III
Thalamus						
Right						
Fractional anisotropy	NS	NS	P<0.05	NS	NS	NS
Apparent diffusion coefficient	NS	NS	NS	NS	NS	NS
Left						
Fractional anisotropy	NS	NS	NS	NS	P<0.05	NS
Apparent diffusion coefficient	NS	NS	P<0.05	NS	NS	NS
Basal ganglia						
Right						
Fractional anisotropy	NS	NS	P<0.05	NS	NS	NS
Apparent diffusion coefficient	NS	NS	P<0.05	NS	NS	NS
Left						
Fractional anisotropy	NS	NS	NS	NS	NS	NS
Apparent diffusion coefficient	NS	NS	P<0.05	NS	NS	NS
Posterior limb of internal capsule						
Right						
Fractional anisotropy	P<0.05	NS	P<0.001	NS	NS	NS
Apparent diffusion coefficient	NS	NS	NS	NS	NS	NS
Left						
Fractional anisotropy	NS	NS	P<0.001	NS	NS	NS
Apparent diffusion coefficient	NS	NS	NS	NS	NS	NS
Cerebral peduncle						
Right						
Fractional anisotropy	P<0.05	NS	P<0.001	NS	NS	NS
Apparent diffusion coefficient	NS	NS	NS	NS	NS	NS
Left						
Fractional anisotropy	NS	NS	NS	NS	NS	NS
Apparent diffusion coefficient	NS	NS	NS	NS	NS	NS
Corticospinal tracts						
Right						
Fractional anisotropy	NS	NS	P<0.05	NS	NS	NS

Contd...

Table 4: Contd...

Parameter	Control vs. Stage I	Control vs. Stage II	Control vs. Stage III	Stage I vs. Stage II	Stage I vs. Stage III	Stage II vs. Stage III
Apparent diffusion coefficient Left	NS	$P < 0.05$	$P < 0.001$	NS	$P < 0.05$	NS
Fractional anisotropy	NS	NS	$P < 0.05$	NS	NS	NS
Apparent diffusion coefficient Frontal	NS	$P < 0.05$	$P < 0.001$	NS	NS	NS
Right						
Fractional anisotropy	NS	NS	$P < 0.05$	NS	NS	NS
Apparent diffusion coefficient Left	NS	NS	$P < 0.001$	NS	$P < 0.05$	NS
Fractional anisotropy	NS	NS	$P < 0.05$	NS	NS	NS
Apparent diffusion coefficient Parietal	NS	NS	$P < 0.001$	NS	NS	NS
Right						
Fractional anisotropy	NS	NS	$P < 0.05$	NS	NS	NS
Left						
Fractional anisotropy	NS	NS	NS	NS	NS	NS
Apparent diffusion coefficient Temporal	NS	$P < 0.05$	$P < 0.001$	NS	$P < 0.001$	NS
Right						
Fractional anisotropy	NS	NS	$P < 0.05$	NS	$P < 0.05$	NS
Apparent Diffusion Coefficient Left	NS	$P < 0.05$	$P < 0.001$	NS	$P < 0.05$	NS
Fractional anisotropy	NS	NS	NS	NS	$P < 0.05$	NS
Apparent diffusion coefficient Occipital	NS	$P < 0.05$	$P < 0.001$	NS	$P < 0.05$	NS
Right						
Fractional anisotropy	NS	NS	NS	NS	NS	NS
Apparent diffusion coefficient Left	NS	$P < 0.05$	$P < 0.001$	NS	$P < 0.05$	NS
Fractional anisotropy	NS	NS	NS	NS	NS	NS
Apparent diffusion coefficient	NS	$P < 0.05$	$P < 0.001$	NS	$P < 0.05$	NS

NS: Non-significant

Diffusion MRI permits biological tissue structure to be probed and imaged on a microscopic scale non-invasively.^[18] Because water diffuses more easily in the direction of the fibers than orthogonally, where it is hindered by myelin sheaths or axonal membranes, this technique has been used to study the organization of the adult WM in fiber bundles.^[19]

In DTI, the ADC and diffusion anisotropy indices such as FA are used to estimate the tissue integrity by analysis of the magnitude of the diffusion of water molecules and their mobility and their deviation from the isotropic diffusion.^[20-21] The ADC usually defined as the ratio of mean-squared displacement and the diffusion time. The ADC value can increase in some forms of pathology, particularly vasogenic edema or accumulation of cellular debris from axonal damage. Therefore, decrement of either FA value and increment of ADC value may indicate injury of the neural tract. Anisotropy values are reduced

in WM damaged areas of brain. Disruptions of integrity for a neural tract also appear to indicate injury of the neural tract.

Changes in anisotropy involving both anisotropy measurements and vector maps will likely prove especially relevant in premature infants, who tend to sustain injury to WM. In the chronic stage of periventricular leukomalacia (PVL), reductions in relative anisotropy may be present, and vector maps may show disruption of WM tracts distant from the focal, cystic lesions detected by conventional imaging. In this case, changes in anisotropy are detectable not only near the site of primary injury, but also in the posterior limb of the internal capsule, indicating a disturbance of developing fibers which project through this area.

Previous studies have proved that early neurologic outcome in neonates with HIE is associated with lower FA

and higher ADC values in specific areas of white or gray matter.^[22-25] During the first week of hypoxic injury, FA values will decrease with both severe and moderate injury as assessed by conventional imaging, whereas ADC values were reduced only in severe injury. Abnormal ADC values pseudo-normalized during the second week and increased after that in chronic phase, whereas FA values continued to decrease.^[26] ADC varies with age also in HIE. In a study neonates who showed areas of reduced ADC were younger at the time imaging (median age 5.5 days, range 2–11 days). The median age was higher in subjects who had normal ADC values (median age 7 days, range, 4–10 days). Those with areas of increased ADC were even older (median age 9.3 days, range, 7–11 days). The age wise differences in ADC were not statistically significant.^[27] So, in previous few studies when the study was done early at day 4–7 after birth a significant decrease in ADC values was observed in asphyxia.^[28] The cause of raised ADC in our study could be due to higher mean age.

DTI can be a qualified biomarker for the early evaluation of neuroprotective interventions as well as for prognosis.^[29-33] Porter *et al.*, (2010) performed DTMRI using 3T in eight healthy control infants, 10 untreated, and 10 hypothermia-treated infants with neonatal encephalopathy with median postnatal age at scan was 1 day (range 1–21) in the healthy infants, 6 days (range 4–20) in the cooled, and 7 days (range 4–18) in non-cooled infants. The authors found that FA was significantly reduced in several WM tracts, anterior and posterior limbs of the internal capsule, corpus callosum, and optic radiations not only in the noncooled infants, but also in the internal capsule in the cooled group. Noncooled infants had significantly lower FA than the cooled treated infants.^[34] Ancora *et al.*, (2013) studied effect of brain cooling in moderate to severely affected hypoxic neonates and performed brain MRI and DTMRI to predict whether DTMRI is a better early predictor of brain damage. The authors found that the decrement of FA was maximum in the frontal and parietal WM, but they did not find any difference to predict early injury in brain using DTMRI.^[35] Lemmon *et al.* demonstrated early changes in DTI in cerebellar region in hypoxic newborn, which is a very late finding via conventional neuroimaging modalities.^[36] In a study conducted by ZHANG *et al.*, demonstrated that DTI provides sensitive detection and early diagnosis of WM injuries in premature infants with HIE.^[37]

Conclusion

The extent of brain injury after perinatal asphyxia was measured by DTMRI. On DTMRI analysis, a decrease in FA and increase in ADC was observed in all ROI in HIE compared to controls. ADC was decreased in asphyxia in some studies also, but no definite values are known depending on the day and extent of injury. Further studies may be required to know the correlation of ADC and day

of life in asphyxiated newborns. Till now, no studies have been done which compared different stages of asphyxia. In our study the differences were most marked in stage III HIE.

Financial support and sponsorship

Nil.

Conflicts of interest

There are no conflicts of interest.

References

- Whitelaw A, Thoresen M. Clinical trials of treatments after perinatal asphyxia. *Curr Opin Pediatr* 2002;14:664-8.
- Shankaran S, Laptook AR. Hypothermia as a treatment for birth asphyxia. *Clin Obstet Gynecol* 2007;50:624-35.
- Gonzalez FF, Ferriero DM. Therapeutics for neonatal brain injury. *Pharmacol Ther* 2008;120:43-53.
- Rennie JM, Leigh B. The legal framework for end-of-life decisions in the UK. *Semin Fetal Neonatal Med* 2008;13:296-300.
- Odd DE, Lewis G, Whitelaw A, Gunnell D. Resuscitation at birth and cognition at 8 years of age: A cohort study. *Lancet* 2009;373:1615-22.
- Rutherford MA, Cowan FM, Manzur AY, Dubowitz LM, Pennock JM, Hajnal JV, *et al.* MR imaging of anisotropically restricted diffusion in the brain of neonates and infants. *J Comput Assist Tomogr* 1991;15:188-98.
- Sakuma H, Nomura Y, Takeda K, Tagami T, Nakagawa T, Tamagawa Y, *et al.* Adult and neonatal human brain: Diffusional anisotropy and myelination with diffusion-weighted MR imaging. *Radiology* 1991;180:229-33.
- Neil JJ, Miller J, Mukherjee P, Huppi PS. Diffusion tensor imaging of normal and injured developing human brain-A technical review. *NMR Biomed* 2002;15:543-52.
- Ralph Heinz E, James MP. Imaging findings in neonatal hypoxia: A practical review. *Am J Roentgenol* 2009;192:41-7.
- Fenichel GM. Hypoxic ischemic encephalopathy in the newborn. *Arch Neurol* 1983;40:261-6.
- Ferriero DM. Neonatal brain injury. *N Engl J Med* 2004;351:1985-95.
- Ferriero DM, Miller SP. Imaging selective vulnerability in the developing nervous system. *J Anat* 2010;229:43-55.
- Yoshiura T, Wu O, Zaheer A, Reese TG, Sorensen AG. Highly diffusion-sensitized MRI of brain: Dissociation of gray and white matter. *Magn Reson Med* 2001;45:734-40.
- Chahboune H, Ment LR, Stewart WB, Rothman DL, Vaccarino FM, Hyder F, *et al.* Hypoxic injury during neonatal development in murine brain: Correlation between *in vivo* DTI findings and behavioral assessment. *Cereb Cortex* 2009;19:2891-901.
- Yakovlev PI, Lecours AR. The myelogenetic cycles of regional maturation of the brain. In: Minkowski A, editor. *Regional development of the brain in early life*. Oxford: Blackwell Scientific; 1967. p. 3-70.
- Brody BA, Kinney HC, Kloman AS, Gilles FH. Sequence of central nervous system myelination in human infancy: I. An autopsy study of myelination. *J Neuropathol Exp Neurol* 1987;46:283-301.
- Miller SP, Vigneron DB, Henry RG, Bohland MA, Ceppi-Cozzio C, Hoffman C, *et al.* Serial quantitative diffusion tensor MRI of the premature brain: Development in newborns with and without injury. *J Magn Reson Imaging* 2002;16:621-32.
- Le Bihan D, Breton E, Lallemand D, Grenier P, Cabanis E,

- Laval-Jeantet M. MR imaging of intravoxel incoherent motions: Application to diffusion and perfusion in neurologic disorders. *Radiology* 1986;161:401-7.
19. Moseley ME, Cohen Y, Kucharczyk J, Mintorovitch J, Asgari HS, Wendland MF, *et al.* Diffusion-weighted MR imaging of anisotropic water diffusion in cat central nervous system. *Radiology* 1990;176:439-45.
 20. Thornton JS, Ordidge RJ, Penrice J, Cady EB, Amess PN, Punwani S, *et al.* Anisotropic water diffusion in white and gray matter of the neonatal piglet brain before and after transient hypoxia-ischaemia. *Magn Res Imag* 1997;15:433-40.
 21. Basser PJ, Mattiello J, Le Bihan D. MR diffusion tensor spectroscopy and imaging. *Biophys J* 1994;66:259-67.
 22. Brissaud O, Amirault M, Villega F, Periot O, Chateil JF, Allard M. Efficiency of fractional anisotropy and apparent diffusion coefficient on diffusion tensor imaging in prognosis of neonates with hypoxic-ischemic encephalopathy: A methodologic prospective pilot study. *AJNR Am J Neuroradiol* 2010;31:282-7.
 23. Wolf RL, Zimmerman RA, Clancy R, Haselgrove JH. Quantitative apparent diffusion coefficient measurements in term neonates for early detection of hypoxicischemic brain injury: Initial experience. *Radiology* 2001;218:825-33.
 24. Rutherford M, Counsell S, Allsop J, Boardman J, Kapellou O, Lartkman D, *et al.* Diffusion weighted magnetic resonance imaging interperinatal brain injury: A comparison with site of lesion and time from birth. *Pediatrics* 2004;114:1004-14.
 25. Hanrahan JD, Cox IJ, Azzopardi D, Cowan FM, Bryant DJ, Edwards AD, *et al.* Relation between proton magnetic resonance spectroscopy within 18 hours of birth asphyxia and neurodevelopment at 1 year of age. *Dev Med Child Neurol* 1999;41:76-82.
 26. Ward P, Counsell S, Allsop J, Cowan F, Shen Y, Edwards D, *et al.* Reduced fractional anisotropy on diffusion tensor magnetic resonance imaging after hypoxic-ischemic encephalopathy. *Pediatrics* 2006;117:e619-30.
 27. Forbes KP, Pipe JG, Bird R. Neonatal hypoxic-ischemic encephalopathy: Detection with diffusion-weighted MR Imaging. *AJNR Am J Neuroradiol* 2000;21:1490-6.
 28. Tusor N, Wusthoff C, Smee N, Merchant N, Arichi T, Edwards AD, *et al.* Prediction of neurodevelopmental outcome after hypoxic-ischemic encephalopathy treated with hypothermia by diffusion tensor imaging analyzed using tract-based spatial statistics. *Pediatr Res* 2012;72:63-9.
 29. Cowan FM, Pennock JM, Hanrahan JD, Manji KP, Edwards AD, *et al.* Early detection of cerebral infarction and hypoxic ischemic encephalopathy in neonates using diffusion weighted magnetic resonance imaging. *Neuropediatrics* 1994;25:172-5.
 30. Dudink J, Mercuri E, Al Nakib L, Govaert P, Counsell SJ, Rutherford MA, *et al.* Evolution of Unilateral perinatal arterial ischemic stroke on conventional and diffusion-weighted mr imaging. *AJNR Am J Neuroradiol* 2009;30:998-1004.
 31. Adams E, Chau V, Poskitt KJ, Grunau RE, Synnes A, Miller SP. Tractography-based quantification of corticospinal tract development in premature newborns. *J Pediatr* 2010;156:882-8.
 32. Bax M, Tydeman C, Flodmark O. Clinical and MRI correlates of cerebral palsy: The European cerebral palsy study. *JAMA* 2006;296:1602-8.
 33. Murakami A, Yamada K, Morimoto M, Kizu O, Nishimura A, Nishimura T, *et al.* Fiber-tracking techniques can predict degree of neurologic impairment for periventricular leukomalacia. *Pediatrics* 2008;122:500-6.
 34. Porter EJ, Counsell SJ, Edwards AD, Allsop J, Azzopardi D. Tract-based spatial statistics of magnetic resonance images to assess disease and treatment effects in perinatal asphyxial encephalopathy. *Pediatr Res* 2010;68:205-9.
 35. Ancora G, Testa C, Grandi S, Tonon C, Sbravati F, Lodi R, *et al.* Prognostic value of brain proton MR spectroscopy and diffusion tensor imaging in newborns with hypoxic-ischemic encephalopathy treated by brain cooling. *Neuroradiology* 2013;55:1017-25.
 36. Lemmon ME, Wagner MW, Bosemani T, Carson KA, Northington FJ, Huisman TA, *et al.* Diffusion tensor imaging detects occult cerebellar injury in severe neonatal hypoxic-ischemic encephalopathy. *Dev Neurosci* 2017.
 37. Zhang F, Liu C, Qian L, Hou H, Guo Z. Diffusion tensor imaging of white matter injury caused by prematurity-induced hypoxic-ischemic brain damage. *Med Sci Monit* 2016;22:2167-74.